

---

# Provably Robust Detection of Out-of-distribution Data (almost) for free

---

**Alexander Meinke\***  
University of Tübingen

**Julian Bitterwolf**  
University of Tübingen

**Matthias Hein**  
University of Tübingen

## Abstract

When applying machine learning in safety-critical systems, a reliable assessment of the uncertainty of a classifier is required. However, deep neural networks are known to produce highly overconfident predictions on out-of-distribution (OOD) data and even if trained to be non-confident on OOD data one can still adversarially manipulate OOD data so that the classifier again assigns high confidence to the manipulated samples. In this paper we propose a novel method where from first principles we combine a certifiable OOD detector with a standard classifier into an OOD aware classifier. In this way we achieve the best of two worlds: certifiably adversarially robust OOD detection, even for OOD samples close to the in-distribution, without loss in prediction accuracy and close to state-of-the-art OOD detection performance for non-manipulated OOD data. Moreover, due to the particular construction our classifier provably avoids the asymptotic overconfidence problem of standard neural networks.

## 1 Introduction

Deep neural networks have achieved state-of-the-art performance in many application domains. However, the widespread usage of deep neural networks in safety-critical applications, e.g. in healthcare, autonomous driving/aviation, manufacturing, raises concerns as deep neural networks have problematic deficiencies. Among these deficiencies are overconfident predictions on non-task related inputs (38; 18; 17) which has recently attracted a lot of interest. ReLU networks have even been shown to be provably overconfident far away from the training data (17). However, reliable confidences of the classifier on the actual classification task (in distribution) (16) as well as on the out-distribution (18; 17) are important to be able to detect when the deep neural network is working outside of its specification, which can then be used to either involve a human operator, e.g. a physician for a medical diagnosis system, or to fall back into a “safe state” in autonomous driving/aviation. Thus, solving this problem is of high importance for trustworthy ML systems.

Many approaches have been proposed for OOD detection, (18; 30; 28; 29; 19; 42; 17; 35; 9; 40) and one of the currently best performing methods enforces low confidence during training on a large and diverse set of out-distribution images (19) which leads to strong separation of in- and out-distribution based on the confidence of the classifier. Crucially, this also generalizes to novel test out-distributions.

However, current OOD detection methods are vulnerable to adversarial manipulations, i.e. small adversarial modifications of OOD inputs lead to large confidence of the classifier on the manipulated samples (38; 17; 44). While different methods for adversarially robust OOD detection have been proposed (17; 44; 35; 9; 6) there is little work on *provably* robust OOD detection (35; 6; 22; 4).

In (35) they append density estimators based on Gaussian mixture models for in- and out-distribution to the softmax layer. By also enforcing low confidence on a training out-distribution, they achieve similar OOD detection performance to (19) but can guarantee that the classifier shows decreasing

---

\*Corresponding author - [alexander.meinke@uni-tuebingen.de](mailto:alexander.meinke@uni-tuebingen.de)

Table 1: **ProoD combines desirable properties of existing (robust) OOD detection methods.** It has high test accuracy and standard OOD detection performance (as (19)) even for close out-distributions (e.g. CIFAR10 vs. CIFAR100) and has worst-case guarantees if the out-distribution samples are adversarially perturbed in an  $l_\infty$ -neighborhood to maximize the confidence. Similar to CCU (35) it avoids the problem of asymptotic overconfidence far away from the training data.

	OE (19)	CCU (35)	ATOM (9)	GOOD (6)	ProoD
High accuracy	✓	✓	✓		✓
High clean OOD	✓	✓	✓		✓
Adv. OOD $l_\infty$ -robustness			(✓)	✓	✓
Adv. OOD $l_\infty$ -certificates				✓	✓
Provably not asympt. overconfident		✓			✓

confidence as one moves away from the training data. However, for close in-distribution inputs this approach yields no guarantee as the Gaussian mixture models are not powerful enough for complex image classification tasks. In (24; 25) similar asymptotic guarantees are derived for Bayesian neural networks but without any robustness guarantees. In (22) they apply randomized smoothing to obtain guarantees wrt to  $l_2$ -perturbations for Dirichlet-based models (33; 34; 45) which already show quite some gap in terms of AUC-ROC to SOTA OOD detection methods even without attacks. Interval bound propagation (IBP) (15; 36; 50; 20) has been shown to be one of the most effective techniques in certified adversarial robustness on the in-distribution when applied during training. In (6) they use IBP to compute upper bounds on the confidence in an  $l_\infty$ -neighborhood of the input and minimize these upper bounds on the training out-distribution. This yields classifiers with pointwise guarantees for robust OOD detection even for “close” out-distribution inputs which generalize to novel OOD test distributions. However, the employed architectures of the neural network are restricted to rather shallow networks as otherwise the bounds of IBP are loose. Thus, they obtain a classification accuracy which is far away from the state-of-the-art, e.g. 91% on CIFAR-10, and thus the approach does not scale to more complex tasks like ImageNet. In particular, despite its low accuracy the employed network architecture is quite large and has higher memory consumption than a ResNet50. Moreover, one does not get any guarantees on the asymptotic behavior of the classifier as one moves away from the training data. The authors of (4) use SOTA verification techniques (13) and get guarantees for OOD detection wrt to  $l_\infty$ -perturbations for ACET models (17) that were not specifically trained to be verifiable but the guarantees obtained by training the models via IBP in (6) are significantly better.

In this paper we propose a framework which merges a certified binary classifier for in-versus out-distribution with a classifier for the in-distribution task in a principled fashion into a joint classifier which combines the advantages of (35) and (6) but does not suffer from the downsides of the respective approaches. In particular, our method simultaneously achieves the following properties:

- Point-wise  $l_\infty$ -robust OOD detection with guarantees similar to (6).
- It provably prevents the asymptotic overconfidence of deep neural networks.
- It can be used with arbitrary architectures and has no loss in prediction performance and standard OOD detection performance.

Thus, we get provable guarantees for robust OOD detection, fix the asymptotic overconfidence (almost) for free as we have (almost) no loss in prediction and standard OOD detection performance. We qualitatively compare the properties of our model to prior approaches in Table 1.

## 2 Provably Robust Detection of Out-of-distribution Data

### 2.1 Notation

In the following we consider feedforward networks for classification,  $f : \mathbb{R}^d \rightarrow \mathbb{R}^K$ , with  $K$  classes defined with  $x^{(0)} = x$  as

$$x^{(l)} = \sigma^{(l)} \left( W^{(l)} x^{(l-1)} + b^{(l)} \right) \quad l = 1, \dots, L-1, \quad f(x) = W^{(L)} x^{(L-1)} + b^{(L)}, \quad (1)$$

where  $L \in \mathbb{N}$  is the number of layers,  $W^{(l)}$  and  $b^{(l)}$  are weights and biases and  $\sigma^{(l)}$  is either the ReLU or leaky ReLU activation function of layer  $l$ . We refer to the output of  $f$  as the *logits* and get

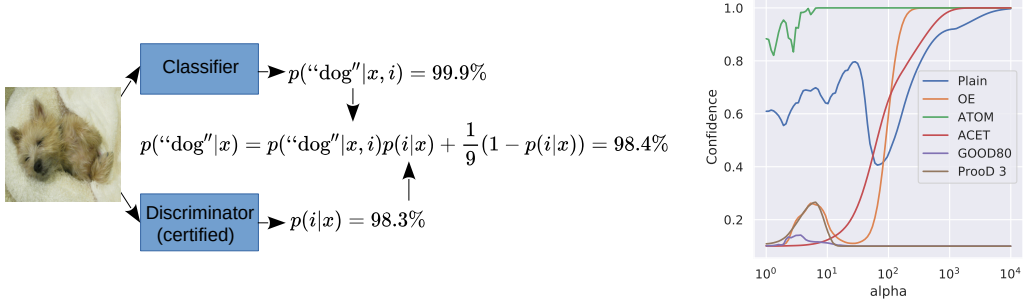


Figure 1: **Left, ProoD:** Our method combines a provable binary discriminator between in- and out-distribution with a standard classifier. **Right, Asymptotic confidence:** We plot the mean confidence in the predicted in-distribution class for different models as one moves away from the center of the box  $[0, 1]^d$  by  $\alpha$  multiples for 10 fixed vectors  $n_i$  (adversarially found for ATOM, see App. A for details). Plain, OE and ACET become asymptotically over-confident as expected by the result of (17). However, as shown in Theorem 1, under mild assumptions our ProoD asymptotically converges to uniform confidence. GOOD80 (6) also converges to uniform confidence along these directions even though no guarantee was shown in (6).

a probability distribution over the classes via  $\hat{p}(y|x) = \frac{e^{f_y(x)}}{\sum^K e^{f_k(x)}}$  for  $y = 1, \dots, K$ . We define the confidence as  $\text{Conf}(f(x)) = \max_{y=1, \dots, K} \hat{p}(y|x)$ .

## 2.2 Joint Model for OOD Detection and Classification

In our joint model we assume that there exists an in- and out-distribution where we assume that out-distribution samples are unrelated to the in-distribution task. Thus we can formally write the conditional distribution on the input as

$$\hat{p}(y|x) = \hat{p}(y|x, i)\hat{p}(i|x) + \hat{p}(y|x, o)\hat{p}(o|x), \quad (2)$$

where  $\hat{p}(i|x)$  is the conditional distribution that sample  $x$  belongs to the in-distribution and  $\hat{p}(y|x, i)$  is the conditional distribution for the in-distribution. We assume that OOD samples are unrelated and thus maximally un-informative to the in-distribution task, i.e. we fix  $\hat{p}(y|x, o) = \frac{1}{K}$ . In (35) they further decomposed  $\hat{p}(i|x) = \frac{\hat{p}(x|i)\hat{p}(i)}{\hat{p}(x)}$  and used Gaussian mixture models to estimate  $\hat{p}(x|i)$  with fixed  $\hat{p}(i) = \hat{p}(o) = \frac{1}{2}$ . As the properties of the Gaussian mixture model can be directly controlled in comparison to a more powerful generative model such as VAEs, this allowed (35) to prove that  $\hat{p}(y|x)$  becomes uniform over the classes if  $x$  is far away from the training data. However, the downside of the Gaussian mixture models is that this approach yields no guarantees for close out-distribution samples. Instead in this paper we directly learn  $\hat{p}(i|x)$  which results in a binary classification problem and we train this binary classifier in a certified robust fashion wrt to an  $l_\infty$ -threat model so that even adversarially manipulated OOD samples are detected. Around  $x \in \mathbb{R}^d$  we have the upper bound

$$\max_{\|u-x\|_\infty \leq \epsilon} \hat{p}(y|u) \leq \max_{\|u-x\|_\infty \leq \epsilon} \hat{p}(i|u) + \frac{1}{K}(1 - \hat{p}(i|u)) = \frac{K-1}{K} \max_{\|u-x\|_\infty \leq \epsilon} \hat{p}(i|u) + \frac{1}{K}, \quad (3)$$

so we can defer the certification ‘‘work’’ to the binary discriminator. Using a particular constraint on the weights of the binary discriminator, we get similar asymptotic properties as in (35) but additionally get certified adversarial robustness for close out-distribution samples as in (6). In contrast to (6) this comes without loss in test accuracy or non-adversarial OOD detection performance as in our model the neural network used for the in-distribution classification task  $\hat{p}(y|x, i)$  is independent of the binary discriminator. Thus, we have the advantage that the classifier can use arbitrary deep neural networks and is not constrained to certifiable networks. We call our approach **Provable out-of-Distribution detector (ProoD)** and visualize its components in Figure 1.

**Certifiably Robust Binary Discrimination of In- versus Out-Distribution** The first goal is to get a certifiably robust OOD detector  $\hat{p}(i|x)$ . We train this binary discriminator independent of the overall classifier as the training schedules for certified robustness are incompatible with the standard training schedules of normal classifiers. For this binary classification problem we use a logistic

model  $\hat{p}(i|x) = \frac{1}{1+e^{-g(x)}}$ , where  $g : \mathbb{R}^d \rightarrow \mathbb{R}$  are logits of a neural network (we denote the weights and biases of  $g$  by  $W_g$  and  $b_g$  in order to discriminate it from the classifier  $f$  introduced in the next paragraph). Let  $(x_r, y_r)_{r=1}^N$  be our in-distribution training data (we use the class encoding  $+1$  for the in-distribution and  $-1$  for out-distribution) and  $(z_s)_{s=1}^M$  be our training out-distribution data. Then the optimization problem associated to the binary classification problem becomes:

$$\min_{W_g^{(L_g)} < 0} \frac{1}{N} \sum_{r=1}^N \log \left( 1 + e^{-g(x_r)} \right) + \frac{1}{M} \sum_{s=1}^M \log \left( 1 + e^{\bar{g}(z_s)} \right), \quad (4)$$

where we minimize over the parameters of the neural network  $g$  under the constraint that the weights of the output layer  $W_g^{(L_g)}$  are componentwise negative and  $\bar{g}(z) \geq \max_{u \in B_p(z, \epsilon)} g(u)$  is an upper bound on the output of  $g$  around OOD samples for a given  $l_p$ -threat model  $B_p(z, \epsilon) = \{u \in [0, 1]^d \mid \|u - z\|_p \leq \epsilon\}$ . In this paper we always use an  $l_\infty$ -threat model. This upper bound could, in principle, be computed using any certification technique but we will use interval bound propagation (IBP) since it is simple, fast and has been shown to produce SOTA results (15). Note that this is not standard adversarial training for a binary classification problem as here we have an asymmetric situation: we want to be (certifiably) robust wrt to adversarial manipulation on the out-distribution data but *not* on the in-distribution and thus the upper bound is only used for out-distribution samples. The negativity constraint on the weights of the output layer  $W_g^{(L_g)}$  is enforced by using the parameterization  $(W_g^{(L_g)})_j = -e^{h_j}$  componentwise and optimizing over  $h_j$ . Later on, the negativity of  $W_g^{(L_g)}$  allows us to control the asymptotic behavior of the joint classifier, see Section 3.

For the reader's convenience we quickly present the upper  $\bar{x}^{(l)}$  and lower  $\underline{x}^{(l)}$  bounds on the output of layer  $l$  in a feedforward neural network produced by IBP:

$$\bar{x}^{(l)} = \sigma \left( W_+^{(l)} \bar{x}^{(l-1)} + W_-^{(l)} \underline{x}^{(l-1)} + b^{(l)} \right), \quad \underline{x}^{(l)} = \sigma \left( W_+^{(l)} \underline{x}^{(l-1)} + W_-^{(l)} \bar{x}^{(l-1)} + b^{(l)} \right), \quad (5)$$

where  $W_+ = \max(0, W)$  and  $W_- = \min(0, W)$  (min/max used componentwise). For an  $l_\infty$ -threat model one starts with the upper and lower bounds for the input layer  $\bar{x}^{(0)} = x + \epsilon$  and  $\underline{x}^{(0)} = x - \epsilon$  and then iteratively computes the layerwise upper and lower bounds  $\bar{x}^{(l)}, \underline{x}^{(l)}$  which fulfill

$$\underline{x}^{(l)} \leq \min_{\|u-x\|_\infty \leq \epsilon} x^{(l)}(u) \leq \max_{\|u-x\|_\infty \leq \epsilon} x^{(l)}(u) \leq \bar{x}^{(l)}. \quad (6)$$

While in (6) they also used IBP to upper bound the confidence of the classifier this resulted in a bound that took into account all  $\mathcal{O}(K^2)$  logit differences between all classes. In contrast, our loss in Eq. (4) is significantly simpler as we just have a binary classification problem and therefore only need a single bound. Thus, our approach easily scales to tasks with a large number of classes and training the binary discriminator with IBP turns out to be significantly more stable than the approach in (6) and does not require many additional tricks.

**(Semi)-Joint Training of the final Classifier** Given the certifiably robust model  $\hat{p}(i|x)$  for the binary classification task between in- and out-distribution, we need to determine the final predictive distribution  $\hat{p}(y|x)$  in Eq. (2). On top of the provable OOD performance that we get from Eq. (3), we also want to achieve SOTA performance on unperturbed OOD data. In principle we could independently train a model for the predictive in-distribution task  $\hat{p}(y|x, i)$ , e.g. using outlier exposure (19) or any other state-of-the-art OOD detection method and simply combine it with our  $\hat{p}(i|x)$ . While this does lead to models with high OOD performance that also have guarantees, it completely ignores the interaction between  $\hat{p}(i|x)$  and  $\hat{p}(y|x, i)$  during training. Instead we propose to train  $\hat{p}(y|x, i)$  by optimizing our final predictive distribution  $\hat{p}(y|x)$ . Note that in order to retain the guarantees of  $\hat{p}(i|x)$  we only train the parameters of the neural network  $f : \mathbb{R}^d \rightarrow \mathbb{R}^K$  and need to keep  $\hat{p}(i|x)$  resp.  $g$  fixed. Because  $g$  stays fixed we call this semi-joint training. We use outlier exposure (19) for training  $\hat{p}(y|x)$  with the cross-entropy loss and use the softmax-function in order to

obtain the predictive distribution  $\hat{p}_f(y|x, i) = \frac{e^{f_y(x)}}{\sum_k e^{f_k(x)}}$  from  $f$ :

$$\begin{aligned} & \min_f -\frac{1}{N} \sum_{r=1}^N \log(\hat{p}(y_r|x_r)) - \frac{1}{M} \sum_{s=1}^M \frac{1}{K} \sum_{l=1}^K \log(\hat{p}(l|z_s)) \\ &= \min_f -\frac{1}{N} \sum_{i=1}^N \log \left( \hat{p}_f(y_r|x_r, i) \hat{p}(i|x_r) + \frac{1}{K} (1 - \hat{p}(i|x_r)) \right) \\ & \quad - \frac{1}{M} \sum_{s=1}^M \frac{1}{K} \sum_{l=1}^K \log \left( \hat{p}_f(l|z_s, i) \hat{p}(i|z_s) + \frac{1}{K} (1 - \hat{p}(i|z_s)) \right), \end{aligned} \quad (7)$$

where the first term is the standard cross-entropy loss on the in-distribution but now for our joint model for  $\hat{p}(y|x)$  and the second term is the outlier exposure term which enforces uniform confidence on out-distribution samples. In App. B we show that semi-joint training does, in fact, lead to stronger guarantees than separate training.

The loss in Eq. (4) implicitly weighs the in-distribution and worst-case out-distribution equally, which amounts to the assumption  $p(i) = \frac{1}{2} = p(o)$ . This highly conservative choice simplifies training the binary discriminator but may not reflect the expected frequency of OOD samples at test time and in effect means that  $\hat{p}(i|x)$  tends to be quite low. This typically yields good guaranteed AUCs but can have a negative impact on the standard out-distribution performance. In order to better explore the trade-off of guaranteed and standard OOD detection, we repeat the above semi-joint training with different shifts of the offset parameter in the output layer

$$b' = b_g^{(L_g)} + \Delta, \quad (8)$$

where  $\Delta \geq 0$  leads to increasing  $\hat{p}(i|x)$ . This shift may appear post-hoc, but it actually has a direct interpretation in terms of the probabilities  $p(i)$  and  $p(o)$ . Under the assumption that our binary discriminator  $g$  is perfect, that is

$$p(i|x) = \frac{p(x|i)p(i)}{p(x|i)p(i) + p(x|o)p(o)} = \frac{1}{1 + \frac{p(x|o)p(o)}{p(x|i)p(i)}} = \frac{1}{1 + e^{-g(x)}}, \quad (9)$$

then it holds that  $e^{g(x)} = \frac{p(x|i)p(i)}{p(x|o)p(o)}$ . A change of the prior probabilities  $\tilde{p}(i)$  and  $\tilde{p}(o)$  without changing  $p(x|i)$  and  $p(x|o)$  then corresponds to a novel classifier

$$e^{\tilde{g}(x)} = \frac{p(x|i)\tilde{p}(i)}{p(x|o)\tilde{p}(o)} = \frac{p(x|i)p(i)}{p(x|o)p(o)} \frac{p(o)\tilde{p}(i)}{p(i)\tilde{p}(o)} = e^{g(x)} e^\Delta, \quad \text{with } \Delta = \log \left( \frac{p(o)\tilde{p}(i)}{p(i)\tilde{p}(o)} \right). \quad (10)$$

Note that  $\tilde{p}(i) > p(i)$  corresponds to positive shifts. In a practical setting, this parameter can be chosen based on the priors for the particular application. Since no such priors are available in our case we determine a suitable shift by evaluating on the training out-distribution, see Section 4.2 for details. Please note that we explicitly do not train the shift parameter since this way the guarantees would get lost as the classifier implicitly learns a large  $\Delta$  in order to maximize the confidence on the in-distribution. This way the classifier would converge to a normal outlier exposure-type classifier without any guarantees.

### 3 Guarantees on Asymptotic Confidence

We note that a ReLU neural network  $f : \mathbb{R}^d \rightarrow \mathbb{R}^K$  as defined in Eq. (1) using ReLU or leaky ReLU as activation functions, potential max-or average pooling and skip connection yields a piece-wise affine function (1; 17), i.e. there exists a finite set of polytopes  $Q_r \subset \mathbb{R}^d$  with  $r = 1, \dots, R$  such that  $\bigcup_{r=1}^R Q_r = \mathbb{R}^d$  and  $f$  restricted to each of the polytopes is an affine function. Since there are only finitely many polytopes some of them have to extend to infinity and on these ones the neural network is essentially an affine classifier. This fact has been used in (17) to show that ReLU networks are almost always asymptotically overconfident in the sense that if one moves to infinity the confidence of the classifier approaches 1 (instead of converging to  $1/K$  as in these regions the classifier has never seen any data).

The following result taken from (17) basically says that as one moves to infinity by upscaling a vector one eventually ends up in a polytope which extends to infinity.

**Lemma 1** ((17)). *Let  $\{Q_r\}_{r=1}^R$  be the set of convex polytopes on which a ReLU-network  $f : \mathbb{R}^d \rightarrow \mathbb{R}^K$  is an affine function, that is for every  $k \in \{1, \dots, R\}$  and  $x \in Q_k$  there exists  $V^k \in \mathbb{R}^{K \times d}$  and  $c^k \in \mathbb{R}^K$  such that  $f(x) = V^k x + c^k$ . For any  $x \in \mathbb{R}^d$  with  $x \neq 0$  there exists  $\alpha \in \mathbb{R}$  and  $t \in \{1, \dots, R\}$  such that  $\beta x \in Q_t$  for all  $\beta \geq \alpha$ .*

The following theorem now shows that, opposite to standard ReLU networks (17), our proposed joint classifier gets provably less confident in its decisions as one moves away from the training data which is a desired property of any reasonable classifier.

**Theorem 1.** *Let  $x \in \mathbb{R}^d$  with  $x \neq 0$  and let  $g : \mathbb{R}^d \rightarrow \mathbb{R}$  be the ReLU-network of the binary discriminator and denote by  $\{Q_r\}_{r=1}^R$  the finite set of polytopes such that  $g$  is affine on these polytopes which exists by Lemma 1. Denote by  $Q_t$  the polytope such that  $\beta x \in Q_t$  for all  $\beta \geq \alpha$  and let  $x^{(L-1)}(z) = Uz + d$  with  $U \in \mathbb{R}^{n_{L-1} \times d}$  and  $d \in \mathbb{R}^{n_{L-1}}$  be the output of the pre-logit layer of  $g$  for  $z \in Q_t$ . If  $Ux \neq 0$ , then*

$$\lim_{\beta \rightarrow \infty} \hat{p}(y|\beta x) = \frac{1}{K}.$$

See the proof in App. C. In App. A we see that the condition  $Ux \neq 0$  is not restrictive, as in all cases we tested this property it holds for our joint classifier (see Figure 1 for an illustration of the asymptotic confidence of ProoD in comparison to other models). The negativity condition on the weights  $W_g^{(L_g)}$  of the output layer of the in-vs. out-distribution discriminator  $g$  is crucial for the proof. While one might think that this condition is restrictive, we did not encounter any negative influence of this constraint on test accuracy, guaranteed or standard OOD detection performance. Thus the asymptotic guarantees come essentially for free. In (35) they derived non-asymptotic guarantees and it would be relatively easy to also achieve this for the joint classifier via a decay factor for  $\hat{p}(i|x)$  that depends on the distance to the training data but we prefer not to enforce this explicitly.

## 4 Experiments

We compare our ProoD in terms of accuracy and clean and adversarial OOD performance on several datasets with the main competitors.

### 4.1 Training of ProoD

We provide experiments on CIFAR10, CIFAR100 (26) and Restricted Imagenet (R.ImgNet) (48). The latter dataset consists of images from the ILSVRC2012 subset of ImageNet (14; 43) that fit within 9 broader superclasses of animals.

**Training the Binary Discriminator** We train the binary discriminator between in-and out-distribution using the loss in Eq. (4) with the bounds over an  $l_\infty$ -ball of radius  $\epsilon = 0.01$  for the out-distribution following (6). We use relatively shallow CNNs with only 5 layers plus pooling layers, see App. D. For the training out-distribution, we follow previous work and use 80M Tiny Images (46) for CIFAR10 and CIFAR100. There have been concerns over the use of this dataset (5) because of offensive class labels. We emphasize that we do not use any of the class labels. Since all prior work used this dataset for the sake of comparison we also use it. However, we also perform our experiments using a downscaled version of OpenImages (27) as training out-distribution in App. E and we encourage the community to use those models and values for future comparisons. For R.ImgNet we use the ILSVRC2012 train images that do not belong to R.ImgNet as training out-distribution (NotR.ImgNet).

**Semi-Joint Training** For the classifier we use a ResNet18 architecture on CIFAR and a ResNet50 on R.ImgNet. Note that the architecture of our binary discriminator is over an order of magnitude smaller than the one in (6) (11MB instead of 135MB) and thus the the memory overhead for the binary discriminator is less than a third of that of the classifier. All schedules, hardware and hyperparameters are described in App. D. As discussed in Section 2.2 when training the binary discriminator one implicitly assumes that in- and (worst-case) out-distribution samples are equally likely. It seems very unlikely that one would be presented with such a large number of OOD samples in practice but as discussed in Section 2.2, we can adjust the weight of the losses after training the discriminator (but before training the classifier) by shifting the bias  $b_g^{(L_g)}$  in the output layer of the binary discriminator.



Figure 2: **(Provable) OOD performance depends on the bias:** Using CIFAR10 as the in-distribution and the test set of 80M Tiny Images as OOD we plot the test accuracy, AUC and GAUC as a function of the bias shift  $\Delta$  (see Eq. (8)). For small  $\Delta$  the AUCs tend to be worse than for the OE model, but small bias shifts also provide stronger guarantees so some trade-off exists.

We train several ProoD models for binary shifts in  $\{0, 1, 2, 3, 4, 5, 6\}$  and then evaluate the AUC and guaranteed AUC (see 4.2) on a subset of the training out-distribution 80M Tiny Images (resp. NotR.ImgNet). As our goal is to have provable guarantees with minimal or no loss on the standard OOD detection task, we choose among all solutions which have better AUC than outlier exposure (OE) (19) the one with the highest guaranteed AUC on 80M Tiny Images (on CIFAR10/CIFAR100) resp. NotR.ImgNet (on R.ImgNet). If none of the solutions has better AUC than OE on the training out-distribution we take the one with the highest AUC (which never happens). We show the trade-off curves for the example of CIFAR10 in Figure 2. The corresponding figures for CIFAR100 and R.ImgNet can be found in App. D.

## 4.2 Evaluation

**Setup** For OOD evaluation for CIFAR10/100 we use the test sets from CIFAR100/10, SVHN (37), the classroom category of downscaled LSUN (49) (LSUN\_CR) as well as smooth noise as suggested in (17) and described in App. D. For R.ImgNet we use Flowers (39), FGVC Aircraft (32), Stanford Cars (23) and smooth noise as test out-distributions. Since the computation of adversarial AUCs (next paragraph) requires computationally expensive adversarial attacks, we restrict the evaluation on the out-distribution to a fixed subset of 1000 images (300 in the case of LSUN\_CR) for the CIFAR experiments and 400 for the R.ImgNet models. We still use the entire test set for the in-distribution.

**Guaranteed and Adversarial AUC** We use the confidence of the classifier as the feature to discriminate between in- and out-distribution samples. While in standard OOD detection one uses the area under the operator-receiver characteristic (AUC) to measure discrimination of in- from out-distribution, in (6) they introduced the worst-case AUC (WCAUC) which is defined as the minimal AUC one can achieve if all out-distribution samples are allowed to be perturbed to reach maximal confidence within a certain threat model, which in our case is an  $l_\infty$ -ball of radius  $\epsilon$ . The AUC and WCAUC are then defined as:

$$\text{AUC}_f(p_1, p_2) = \mathbb{E}_{\substack{x \sim p_1 \\ z \sim p_2}} [\mathbb{1}_{\text{Conf}(x) > \text{Conf}(z)}], \quad \text{WCAUC}_f(p_1, p_2) = \mathbb{E}_{\substack{x \sim p_1 \\ z \sim p_2}} \left[ \mathbb{1}_{\text{Conf}(x) > \max_{\|u-z\|_\infty \leq \epsilon} \text{Conf}(u)} \right],$$

where  $p_1, p_2$  are in- resp. out-distribution and with slight abuse of notation the indicator function  $\mathbb{1}$  returns 1 if the expression in its argument is true and 0 otherwise. Since the exact evaluation of the WCAUC is computationally infeasible we compute an upper bound on the WCAUC, the adversarial AUC (AAUC), by maximizing the confidence using an adversarial attack inside the  $l_\infty$ -ball and we compute a lower bound on the WCAUC, the guaranteed AUC (GAUC), by using bounds on the confidence inside the  $l_\infty$ -ball via IBP.

Gradient obfuscation (41; 2) poses a significant challenge for the evaluation of AAUCs (6) so we employ an ensemble of different versions of projected gradient descent (PGD) (31). We use APGD (11) (except on RImgNet, due to a memory leak) with 500 iterations and 5 random restarts. We also use a 200-step PGD attack with momentum of 0.9 and backtracking that starts with a step size of 0.1 which is halved every time a gradient step does not increase the confidence and gets multiplied by 1.1 otherwise. This PGD is applied to different starting points: i) a decontrasted version

of the image, i.e. the point that minimizes the  $l_\infty$ -distance to the grey image  $0.5 \cdot \vec{1}$  within the threat model, ii) 3 uniformly drawn samples from the threat model and iii) 3 versions of the original image perturbed by Gaussian noise with  $\sigma = 10^{-4}$  and then clipped to the threat model. We always clip to the box  $[0, 1]^d$  at each step of the attack. Using different types of starting points is crucial for strong attacks on these OOD points, as some models have precisely 0 gradients on many OOD samples.

**Baselines** We compare to a normally trained baseline (Plain) and outlier exposure (OE), both trained using the same architecture and hyperparameters as the classifier in our ProoD. For both ATOM and ACET we use the publicly available pre-trained Densenets from (9) (note that these are only available for CIFAR10/100). For GOOD we use the publicly available models from (6). Since they are only available on CIFAR10, we attempted to train models on CIFAR100 using their code and the same hyperparameters and schedules as they used for CIFAR10. This only lead to models with accuracy below 25%, so we do not include these models in our evaluation. Since CCU was already shown to not provide benefits over OE on OOD data that is not very far from the in-distribution (e.g. uniform noise) (35; 6) we do not include it as a baseline. We also evaluate the OOD-performance of the provable binary discriminator (ProoD-Disc) that we trained for ProoD. Note that this is not a classifier and so it is included simply for reference. All results are shown in Table 2.

**Results** ProoD achieves non-trivial GAUCs on all datasets. As was also observed in (6) this shows that the IBP guarantees not only generalize to unseen samples but even to unseen distributions. In general the gap between our GAUCs and AAUCs is extremely small. This shows that the seemingly simple IBP bounds can be remarkably tight, as has been observed in other works (15; 20). It also shows that there would be very little benefit in applying stronger verification techniques like (10; 21; 13) to our ProoD. The bounds are also much tighter than for GOOD, which is likely due to the fact that the confidence on GOOD is much harder to optimize during an attack because it involves maximizing the confidence in an essentially random class.

ProoD’s GAUCs are higher than the AAUCs of ATOM on every evaluated dataset and thus ProoD is *provably better* at the task than ATOM. This may seem surprising because the authors of (9) claimed far stronger adversarial OOD performance on the much harder threat model of  $\epsilon = 8/255 > 0.03$  (compared to our  $\epsilon = 0.01$ ). For example, they report an AAUC of 83.78% on CIFAR10 vs. SVHN compared to the 8.6% that we find within the weaker threat model. Similar failures of adversarial robustness on the in the in-distribution are common in the literature (47; 8; 7; 2; 11) and this result shows emphatically why certified adversarial OOD robustness is so important as empirical evaluations can be unreliable. We can see a similar issue with ACET. On CIFAR10 it appears that it is quite robust to our attacks, but on CIFAR100 it fails completely with AAUCs below even those of OE. Evidently the training on CIFAR100 failed, but only very strong attacks can show this. Interestingly, only the non-robust ACET model has no drop in accuracy, corroborating the findings in (3).

On CIFAR10 we see that ProoD’s GAUCs are comparable to, if slightly worse than the ones of GOOD<sub>80</sub> and strictly worse than the GAUCs of GOOD<sub>100</sub>. However, we want to point out that ProoD achieves this while retaining both high accuracy and OOD performance, both of which are lacking for GOOD. It is also noteworthy that the GOOD models’ memory footprints are over twice as large as ProoD’s. Generally, the accuracy and OOD performance of ProoD are comparable to OE. On CIFAR100 the accuracy and the clean AUC against CIFAR10 are somewhat smaller than for OE, by 0.5% and 3.4% respectively. Together with the failure of GOOD to train at all, the failure of ACET to train robustly and the low clean AUCs of ATOM against CIFAR10 (13.4% worse than plain) this may indicate that obtaining OOD robustness on a task with this many classes is very challenging.

To the best of our knowledge with R.ImgNet we provide the first worst case OOD guarantees on high-resolution images. The fact that our GAUCs are much higher than on CIFAR100 and comparable to those on CIFAR10 indicates that meaningful certification on higher resolution is much more achievable on this task than one might have expected. FGVC and Cars may appear to be relatively simple to separate from the animals in R.ImgNet but the same cannot be said for Flowers which can be more difficult to provably distinguish from images of insects that may have flowers in them.

## 5 Limitations

Our work shows that robustness guarantees for OOD detection are possible without loss in performance on the classification task and normal OOD detection. However, the robustness guarantees

Table 2: **OOD performance:** For all models we report accuracy on the test set of the in-distribution and AUCs, guaranteed AUCs (GAUC), adversarial AUCs (AAUC) for different test out-distributions. The radius of the  $l_\infty$ -ball for the adversarial manipulations of the OOD data is  $\epsilon = 0.01$  for all datasets. The bias shift  $\Delta$  that was used for ProoD is shown for each in-distribution. ProoD provides guarantees that are strictly better than ATOM’s empirical performance on the adversarial task, all while retaining the same accuracy as Plain and OE. The AAUCs and GAUCs for ProoD tend to be very close, indicating remarkably tight certification bounds. Note that ATOM and ACET have lower accuracy on CIFAR100, because their architecture is smaller.

In: CIFAR10	CIFAR100			SVHN			LSUN_CR			Smooth			
	Acc	AUC	GAUC	AAUC	AUC	GAUC	AAUC	AUC	GAUC	AAUC	AUC	GAUC	AAUC
Plain	95.01	90.0	0.0	0.6	93.8	0.0	0.1	93.1	0.0	0.5	98.2	0.0	0.6
OE	95.53	96.1	0.0	6.0	99.2	0.0	0.4	99.5	0.0	15.2	99.0	0.0	11.3
ATOM	95.20	93.7	0.0	14.4	99.6	0.0	8.6	99.7	0.0	40.0	99.6	0.0	18.8
ACET	91.48	91.2	0.0	80.5	95.3	0.0	87.6	98.9	0.0	95.0	99.9	0.0	98.3
GOOD <sub>80</sub>	90.13	87.2	42.5	63.9	94.2	37.5	67.4	93.3	55.2	83.6	95.3	57.3	88.5
GOOD <sub>100</sub>	90.14	70.7	54.5	55.0	74.9	56.3	56.6	75.2	61.0	61.6	81.4	66.6	67.5
ProoD-Disc	-	67.4	61.0	61.7	73.2	65.5	66.4	78.0	72.2	72.7	82.3	71.5	72.9
ProoD $\Delta=3$	95.47	96.0	41.9	43.9	99.5	48.8	49.4	99.6	47.6	53.1	99.7	55.8	57.0
In: CIFAR100	CIFAR10			SVHN			LSUN_CR			Smooth			
	Acc	AUC	GAUC	AAUC	AUC	GAUC	AAUC	AUC	GAUC	AAUC	AUC	GAUC	AAUC
Plain	77.38	77.7	0.0	0.3	81.9	0.0	0.2	76.4	0.0	0.3	88.8	0.0	0.5
OE	77.28	83.9	0.0	0.8	92.8	0.0	0.1	97.4	0.0	4.6	97.6	0.0	0.9
ATOM	75.06	64.3	0.0	0.2	93.6	0.0	0.2	97.5	0.0	9.3	98.5	0.0	15.0
ACET	74.43	79.8	0.0	0.2	90.2	0.0	0.0	96.0	0.0	2.1	92.9	0.0	0.3
ProoD-Disc	-	53.8	50.3	50.4	73.1	69.8	69.9	68.1	63.8	64.0	67.2	63.8	63.9
ProoD $\Delta=1$	76.79	80.5	23.1	23.2	93.7	33.9	34.0	97.2	29.6	30.4	98.9	29.7	31.3
In: R.ImgNet	Flowers			FGVC			Cars			Smooth			
	Acc	AUC	GAUC	AAUC	AUC	GAUC	AAUC	AUC	GAUC	AAUC	AUC	GAUC	AAUC
Plain	96.34	92.3	0.0	0.5	92.6	0.0	0.0	92.7	0.0	0.1	98.9	0.0	8.6
OE	97.10	96.9	0.0	0.2	99.7	0.0	0.4	99.9	0.0	1.8	98.0	0.0	1.9
ProoD-Disc	-	81.5	76.8	77.3	92.8	89.3	89.6	90.7	86.9	87.3	81.0	74.0	74.8
ProoD $\Delta=4$	97.25	96.9	57.5	58.0	99.8	67.4	67.9	99.9	65.7	66.2	98.6	52.7	53.5

are not yet useful to guarantee adversarially robust OOD detection in practice as most GAUCs are still below 50% (while this is chance level, we note that this is against an adversary). Therefore, our ProoD-models are unable to give robustness guarantees on false positive rates at 95% true positive rate (however note that our FPRs for unperturbed OOD data are similar to the ones of OE, see App. F). But considering that this paper achieves guarantees (almost) without loss on the actual task, we think that this work also serves as an important stepping stone towards non-trivial guaranteed robust FPR rates. We further note that ProoD does not perform particularly well on uniform noise, as shown in App. G. We find this limitation to be fairly minor, since uniform noise can be easily discerned from the in-distribution by using simple statistical methods.

## 6 Conclusion

We have demonstrated how to combine a provably robust binary discriminator between in- and out-distribution with a standard classifier in order to simultaneously achieve high accuracy, high OOD detection performance as well as worst-case OOD guarantees that are comparable to previous works - thus we have combined the best properties of previous work. We further showed how in our model simply enforcing negativity in the final weights of the discriminator fixes the problem of asymptotic overconfidence in ReLU classifiers. We described how these networks can be trained simply and stably and thus we provide OOD guarantees that come (almost) for free.

## Acknowledgments and Disclosure of Funding

The authors acknowledge support from the German Federal Ministry of Education and Research (BMBF) through the Tübingen AI Center (FKZ: 01IS18039A) and from the Deutsche Forschungsgemeinschaft (DFG, German Research Foundation) under Germany’s Excellence Strategy (EXCnumber 2064/1, Project number 390727645), as well as from the DFG TRR 248 (Project number389792660). The authors thank the International Max Planck Research School for Intelligent Systems (IMPRS-IS) for supporting Alexander Meinke. We also thank Maximilian Augustin for helpful advice.

## References

- [1] R. Arora, A. Basu, P. Mianjyz, and A. Mukherjee. Understanding deep neural networks with rectified linear unit. In *ICLR*, 2018.
- [2] A. Athalye, N. Carlini, and D. Wagner. Obfuscated gradients give a false sense of security: Circumventing defenses to adversarial examples. In *ICML*, 2018.
- [3] M. Augustin, A. Meinke, and M. Hein. Adversarial robustness on in-and out-distribution improves explainability. In *ECCV*, 2020.
- [4] L. Berrada, S. Dathathri, R. Stanforth, R. Bunel, J. Uesato, S. Gowal, M. P. Kumar, et al. Verifying probabilistic specifications with functional lagrangians. *arXiv:2102.09479*, 2021.
- [5] A. Birhane and V. U. Prabhu. Large image datasets: A pyrrhic win for computer vision? In *WACV*, 2021.
- [6] J. Bitterwolf, A. Meinke, and M. Hein. Certifiably adversarially robust detection of out-of-distribution data. *NeurIPS*, 2020.
- [7] N. Carlini and D. Wagner. Adversarial examples are not easily detected: Bypassing ten detection methods. In *ACM Workshop on Artificial Intelligence and Security*, 2017.
- [8] N. Carlini and D. Wagner. Towards evaluating the robustness of neural networks. In *IEEE Symposium on Security and Privacy*, 2017.
- [9] J. Chen, Y. Li, X. Wu, Y. Liang, and S. Jha. Informative outlier matters: Robustifying out-of-distribution detection using outlier mining. *preprint, arXiv:2006.15207*, 2020.
- [10] C.-H. Cheng, G. Nürenberg, and H. Ruess. Maximum resilience of artificial neural networks. In *International Symposium on Automated Technology for Verification and Analysis*, 2017.
- [11] F. Croce and M. Hein. Reliable evaluation of adversarial robustness with an ensemble of diverse parameter-free attacks. In *ICML*, 2020.
- [12] E. D. Cubuk, B. Zoph, D. Mane, V. Vasudevan, and Q. V. Le. Autoaugment: Learning augmentation strategies from data. In *CVPR*, 2019.
- [13] S. Dathathri, K. Dvijotham, A. Kurakin, A. Raghunathan, J. Uesato, R. Bunel, S. Shankar, J. Steinhardt, I. Goodfellow, P. Liang, et al. Enabling certification of verification-agnostic networks via memory-efficient semidefinite programming. In *NeurIPS*, 2020.
- [14] J. Deng, W. Dong, R. Socher, L.-J. Li, K. Li, and L. Fei-Fei. Imagenet: A large-scale hierarchical image database. In *CVPR*, 2009.
- [15] S. Gowal, K. Dvijotham, R. Stanforth, R. Bunel, C. Qin, J. Uesato, R. Arandjelovic, T. Mann, and P. Kohli. On the effectiveness of interval bound propagation for training verifiably robust models. *arXiv:1810.12715*, 2018.
- [16] C. Guo, G. Pleiss, Y. Sun, and K. Weinberger. On calibration of modern neural networks. In *ICML*, 2017.
- [17] M. Hein, M. Andriushchenko, and J. Bitterwolf. Why ReLU networks yield high-confidence predictions far away from the training data and how to mitigate the problem. In *CVPR*, 2019.
- [18] D. Hendrycks and K. Gimpel. A baseline for detecting misclassified and out-of-distribution examples in neural networks. In *ICLR*, 2017.
- [19] D. Hendrycks, M. Mazeika, and T. Dietterich. Deep anomaly detection with outlier exposure. In *ICLR*, 2019.
- [20] N. Jovanović, M. Balunović, M. Baader, and M. Vechev. Certified defenses: Why tighter relaxations may hurt training? *arXiv:2102.06700*, 2021.
- [21] G. Katz, C. Barrett, D. Dill, K. Julian, and M. Kochenderfer. Reluplex: An efficient smt solver for verifying deep neural networks. In *CAV*, 2017.
- [22] A.-K. Kopetzki, B. Charpentier, D. Zügner, S. Giri, and S. Günnemann. Evaluating robustness of predictive uncertainty estimation: Are dirichlet-based models reliable? *arXiv:2010.14986*, 2020.

[23] J. Krause, M. Stark, J. Deng, and L. Fei-Fei. 3d object representations for fine-grained categorization. In *ICCV vision workshop*, 2013.

[24] A. Kristiadi, M. Hein, and P. Hennig. Being Bayesian, Even Just a Bit, Fixes Overconfidence in ReLU Networks. In *ICML*, 2020.

[25] A. Kristiadi, M. Hein, and P. Hennig. Fixing asymptotic uncertainty of bayesian neural networks with infinite relu features. *arXiv:2010.02709*, 2020.

[26] A. Krizhevsky and G. Hinton. Learning multiple layers of features from tiny images. Technical report, Citeseer, 2009.

[27] A. Kuznetsova, H. Rom, N. Alldrin, J. Uijlings, I. Krasin, J. Pont-Tuset, S. Kamali, S. Popov, M. Malloci, A. Kolesnikov, et al. The open images dataset v4. *International Journal of Computer Vision*, 2020.

[28] K. Lee, H. Lee, K. Lee, and J. Shin. Training confidence-calibrated classifiers for detecting out-of-distribution samples. In *ICLR*, 2018.

[29] K. Lee, K. Lee, H. Lee, and J. Shin. A simple unified framework for detecting out-of-distribution samples and adversarial attacks. In *NeurIPS*, 2018.

[30] S. Liang, Y. Li, and R. Srikant. Enhancing the reliability of out-of-distribution image detection in neural networks. In *ICLR*, 2018.

[31] A. Madry, A. Makelov, L. Schmidt, D. Tsipras, and A. Valdu. Towards deep learning models resistant to adversarial attacks. In *ICLR*, 2018.

[32] S. Maji, E. Rahtu, J. Kannala, M. Blaschko, and A. Vedaldi. Fine-grained visual classification of aircraft. *arXiv:1306.5151*, 2013.

[33] A. Malinin and M. Gales. Predictive uncertainty estimation via prior networks. In *NeurIPS*, 2018.

[34] A. Malinin and M. Gales. Reverse kl-divergence training of prior networks: Improved uncertainty and adversarial robustness. In *NeurIPS*, 2019.

[35] A. Meinke and M. Hein. Towards neural networks that provably know when they don't know. In *ICLR*, 2020.

[36] M. Mirman, T. Gehr, and M. Vechev. Differentiable abstract interpretation for provably robust neural networks. In *ICML*, 2018.

[37] Y. Netzer, T. Wang, A. Coates, A. Bissacco, B. Wu, and A. Y. Ng. Reading digits in natural images with unsupervised feature learning. In *NeurIPS Workshop on Deep Learning and Unsupervised Feature Learning*, 2011.

[38] A. Nguyen, J. Yosinski, and J. Clune. Deep neural networks are easily fooled: High confidence predictions for unrecognizable images. In *CVPR*, 2015.

[39] M.-E. Nilsback and A. Zisserman. Automated flower classification over a large number of classes. In *2008 Sixth Indian Conference on Computer Vision, Graphics & Image Processing*, 2008.

[40] A.-A. Papadopoulos, M. R. Rajati, N. Shaikh, and J. Wang. Outlier exposure with confidence control for out-of-distribution detection. *Neurocomputing*, 2021.

[41] N. Papernot, P. McDaniel, I. Goodfellow, S. Jha, Z. B. Celik, and A. Swami. Practical black-box attacks against machine learning. In *ACM ASIACCS*, 2017.

[42] J. Ren, P. J. Liu, E. Fertig, J. Snoek, R. Poplin, M. A. DePristo, J. V. Dillon, and B. Lakshminarayanan. Likelihood ratios for out-of-distribution detection. In *NeurIPS*, 2019.

[43] O. Russakovsky, J. Deng, H. Su, J. Krause, S. Satheesh, S. Ma, Z. Huang, A. Karpathy, A. Khosla, M. Bernstein, A. C. Berg, and L. Fei-Fei. ImageNet Large Scale Visual Recognition Challenge. *International Journal of Computer Vision (IJCV)*, 2015.

[44] V. Sehwag, A. N. Bhagoji, L. Song, C. Sitawarin, D. Cullina, M. Chiang, and P. Mittal. Better the devil you know: An analysis of evasion attacks using out-of-distribution adversarial examples. *preprint, arXiv:1905.01726*, 2019.

[45] M. Sensoy, L. Kaplan, and M. Kandemir. Evidential deep learning to quantify classification uncertainty. In *NeurIPS*, 2018.

[46] A. Torralba, R. Fergus, and W. T. Freeman. 80 million tiny images: A large data set for nonparametric object and scene recognition. *IEEE transactions on pattern analysis and machine intelligence*, 30(11):1958–1970, 2008.

[47] F. Tramer, N. Carlini, W. Brendel, and A. Madry. On adaptive attacks to adversarial example defenses. *arXiv:2002.08347*, 2020.

[48] D. Tsipras, S. Santurkar, L. Engstrom, A. Turner, and A. Madry. Robustness may be at odds with accuracy. In *ICLR*, 2018.

[49] F. Yu, Y. Zhang, S. Song, A. Seff, and J. Xiao. Lsun: Construction of a large-scale image dataset using deep learning with humans in the loop. *CoRR*, abs/1506.03365, 2015.

[50] H. Zhang, H. Chen, C. Xiao, S. Gowal, R. Stanforth, B. Li, D. Boning, and C.-J. Hsieh. Towards stable and efficient training of verifiably robust neural networks. In *ICLR*, 2020.

## Checklist

1. For all authors...
  - (a) Do the main claims made in the abstract and introduction accurately reflect the paper's contributions and scope? **[Yes]**
  - (b) Did you describe the limitations of your work? **[Yes]** We discuss it in Section 5.
  - (c) Did you discuss any potential negative societal impacts of your work? **[No]** We do not see negative societal impacts. Since the paper contributes to the area of trustworthy AI, we rather hope to mitigate existing risks.
  - (d) Have you read the ethics review guidelines and ensured that your paper conforms to them? **[Yes]** We describe in Section 4 that we use the discarded dataset 80Million Tiny Images (46) for comparison to the literature. Crucially, in App. E we additionally use the non-discarded dataset OpenImages (27) as out-distribution for CIFAR10/CIFAR100 and we strongly encourage the community to compare to those results in future work.
2. If you are including theoretical results...
  - (a) Did you state the full set of assumptions of all theoretical results? **[Yes]**
  - (b) Did you include complete proofs of all theoretical results? **[Yes]** The proof to Theorem 1 can be found in App. C.
3. If you ran experiments...
  - (a) Did you include the code, data, and instructions needed to reproduce the main experimental results (either in the supplemental material or as a URL)? **[Yes]**
  - (b) Did you specify all the training details (e.g., data splits, hyperparameters, how they were chosen)? **[Yes]** We discuss the training details in App. D.
  - (c) Did you report error bars (e.g., with respect to the random seed after running experiments multiple times)? **[Yes]** In an effort to be conscious of the resource consumption we only provided error bars for our models on CIFAR10 in App. H.
  - (d) Did you include the total amount of compute and the type of resources used (e.g., type of GPUs, internal cluster, or cloud provider)? **[Yes]** Please refer to App. D.
4. If you are using existing assets (e.g., code, data, models) or curating/releasing new assets...
  - (a) If your work uses existing assets, did you cite the creators? **[Yes]**
  - (b) Did you mention the license of the assets? **[Yes]** Please refer to App. D.
  - (c) Did you include any new assets either in the supplemental material or as a URL? **[N/A]**
  - (d) Did you discuss whether and how consent was obtained from people whose data you're using/curating? **[N/A]**
  - (e) Did you discuss whether the data you are using/curating contains personally identifiable information or offensive content? **[Yes]**
5. If you used crowdsourcing or conducted research with human subjects...
  - (a) Did you include the full text of instructions given to participants and screenshots, if applicable? **[N/A]**
  - (b) Did you describe any potential participant risks, with links to Institutional Review Board (IRB) approvals, if applicable? **[N/A]**
  - (c) Did you include the estimated hourly wage paid to participants and the total amount spent on participant compensation? **[N/A]**

## A Adversarial Asymptotic Overconfidence

According to the authors of (17), under mild conditions, we should expect to find asymptotic overconfidence in all ReLU networks and almost all directions. For Plain, OE and ACET we did indeed observe this. However, the theorem in (17) does not apply to ATOM since it uses an out-class. It can therefore happen that ATOM only ever gets more confident in the out-class as we move further away from the training data. Empirically, this does appear to be true for the majority of directions. However, as shown in Figure 1, it is possible to find directions in which ATOM becomes arbitrarily over-confident in an in-distribution class. The way we found these directions is as follows: We start from a random point  $x \in [-0.5, 0.5]^d$  that we project onto a sphere of radius 100. We now run gradient descent (for 2000 steps), minimizing  $f_{K+1}(x) - \max_{k \in \{1, \dots, K\}} f_k(x)$  while projecting onto the sphere at each step (unnormalized gradients with step size 0.1 for the first 1000 steps and 0.01 for the last 1000 steps). We then increase the radius of the sphere to 1000 and run an additional 2000 steps with a step size of 0.1. The directions that receive high confidence in an in-distribution class by ATOM tend to also remain in-distribution when scaled up by arbitrarily large factors. The mean confidence over 10 such directions is shown in Figure 1.

It is interesting to ask if similar directions can also be found for ProoD. Of course, the architecture provably prevents arbitrarily overconfident predictions and Theorem 1 ensures that most directions will indeed converge to uniform, but it is, in principle, possible to find directions where the confidence  $\hat{p}(i|x)$  remains constant if the condition  $Ux \neq 0$  in Theorem 1 is not satisfied. We attempted to find such directions by running an attack similar to the one described above. But even using as many as 50000 iterations using various schedules for the radius and the step size, we were unable to find directions where the confidence did not become uniform asymptotically. Concretely, consider a similar attack to the above, where we attempt to maximize  $g(x)$  on the surface of a sphere of radius 100 for 10000 steps with step size 0.1 and 10000 steps with step size 0.01. We increase the radius to 1000 and run an additional 20000 steps with step size 0.1. We rescale the resulting direction vector down to an  $l_\infty$ -ball of norm 1 and compute the confidence  $\hat{p}(i|x)$  as a function of the scaling in the adversarial directions. We show the resulting scale-wise *maximum* over 100 adversarial directions in Figure 3. Note that even the worst-case over 100 adversarially found directions decays to 0 asymptotically, thus empirically confirming the practical utility of Theorem 1.

In Figure 1 GOOD also stands out as having low confidence in all directions that we studied. This is because in all the asymptotic regions that we looked at, the pre-activations of the penultimate layer are all negative. If one moves outward and these pre-activations only get more negative in all directions far away from the data, the confidence does, in fact, remain low. Unfortunately, it also leads to gradients that are precisely zero, which is why the same attack can not be applied here. However, there is no guarantee that GOOD does not also get in some direction asymptotically overconfident.

## B Separate Training for ProoD

In Section 2.2 we describe semi-joint training of  $\hat{p}(y|x)$ . However, as pointed out in that section, it is possible to separately train a certifiable binary discriminator  $\hat{p}(i|x)$  and an OOD aware classifier  $\hat{p}(y|x, i)$  and to then simply combine them via Eq. (2). We call this method separate training ProoD-S and evaluate it by using an OE trained model for  $\hat{p}(y|x, i)$ . We show the results in Table 4, where we repeat the results for OE and ProoD for the reader’s convenience. Note that OE and ProoD-S must always have the same accuracy on the in-distribution since they use the same model for classification (note that (2) preserves the ranking of  $\hat{p}(y|x, i)$ ).

We see that the AUCs of ProoD-S are almost identical to those of OE. Without almost any loss in performance ProoD-S manages to provide non-trivial GAUCs. However, as one would expect, the semi-jointly trained ProoD provides stronger guarantees at similar clean performance. Nonetheless, this post-hoc method of adding some amount of certifiability to an existing system may be interesting in applications where retraining a deployed model from scratch is infeasible.

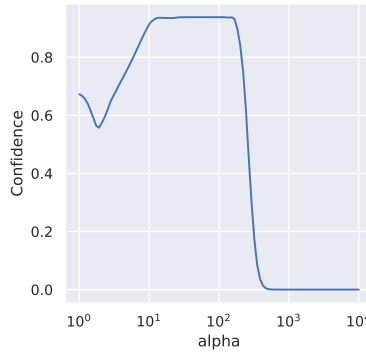


Figure 3: **Plot of  $\hat{p}(i|x)$ , ProoD has low confidence asymptotically:** we plot the maximum of  $\hat{p}(i|x)$  across 100 adversarially chosen directions as one moves further in these directions by factors of  $\alpha$ . Note that  $\hat{p}(i|x) \rightarrow 0$  implies  $\hat{p}(y|x) \rightarrow \frac{1}{K}$ .

Table 3: **Architecture:** The architectures that are used for the binary discriminators. Each convolutional layer is directly followed by a ReLU.

CIFAR	R.ImgNet
Conv2d(3, 128)	Conv2d(3, 128)
Conv2d(128, 256) <sub>s=2</sub>	AvgPool(2)
Conv2d(256, 256)	Conv2d(128, 256) <sub>s=2</sub>
AvgPool(2)	AvgPool(2)
FC(16384, 128)	Conv2d(256, 256)
FC(128, 1)	AvgPool(2)
	FC(50176, 128)
	FC(128, 1)

Table 4: **Separate Training:** Addendum to Table 2 showing the AUCs, GAUCs and AAUCs of ProoD-S on all datasets. The accuracy must always be identical to that of OE and the clean AUCs are also very similar to those of OE. The guarantees are strictly weaker than those provided by the semi-jointly trained ProoD.

In: CIFAR10	CIFAR100			SVHN			LSUN_CR			Smooth			
	Acc	AUC	GAUC	AAUC	AUC	GAUC	AAUC	AUC	GAUC	AAUC	AUC	GAUC	AAUC
OE	95.53	96.1	0.0	6.0	99.2	0.0	0.4	99.5	0.0	15.2	99.0	0.0	11.3
ProoD-S $\Delta=3$	95.53	96.2	28.5	31.8	99.2	33.4	34.7	99.5	32.3	41.0	99.0	31.5	39.7
ProoD $\Delta=3$	95.47	96.0	41.9	43.9	99.5	48.8	49.4	99.6	47.6	53.1	99.7	55.8	57.0
In: CIFAR100	CIFAR10			SVHN			LSUN_CR			Smooth			
	Acc	AUC	GAUC	AAUC	AUC	GAUC	AAUC	AUC	GAUC	AAUC	AUC	GAUC	AAUC
OE	77.28	83.9	0.0	0.8	92.8	0.0	0.1	97.4	0.0	4.6	97.6	0.0	0.9
ProoD-S $\Delta=1$	77.28	83.8	17.8	18.0	93.0	26.7	26.8	97.4	22.9	23.8	97.6	22.9	23.1
ProoD $\Delta=1$	76.79	80.5	23.1	23.2	93.7	33.9	34.0	97.2	29.6	30.4	98.9	29.7	31.3
In: R.ImgNet	Flowers			FGVC			Cars			Smooth			
	Acc	AUC	GAUC	AAUC	AUC	GAUC	AAUC	AUC	GAUC	AAUC	AUC	GAUC	AAUC
OE	97.10	96.9	0.0	0.2	99.7	0.0	0.4	99.9	0.0	1.8	98.0	0.0	1.9
ProoD-S $\Delta=4$	97.10	96.9	50.1	50.7	99.7	59.7	60.6	99.9	57.9	58.9	98.0	40.8	42.3
ProoD $\Delta=4$	97.25	96.9	57.5	58.0	99.8	67.4	67.9	99.9	65.7	66.2	98.6	52.7	53.5

## C Proof of Theorem 1

**Theorem 1.** Let  $x \in \mathbb{R}^d$  with  $x \neq 0$  and let  $g : \mathbb{R}^d \rightarrow \mathbb{R}$  be the ReLU-network of the binary discriminator and denote by  $\{Q_r\}_{r=1}^R$  the finite set of polytopes such that  $g$  is affine on these polytopes which exists by Lemma 1. Denote by  $Q_t$  the polytope such that  $\beta x \in Q_t$  for all  $\beta \geq \alpha$  and let  $x^{(L-1)}(z) = Uz + d$  with  $U \in \mathbb{R}^{n_{L-1} \times d}$  and  $d \in \mathbb{R}^{n_{L-1}}$  be the output of the pre-logit layer of  $g$  for  $z \in Q_t$ . If  $Ux \neq 0$ , then

$$\lim_{\beta \rightarrow \infty} \hat{p}(y|\beta x) = \frac{1}{K}.$$

*Proof.* We note that with a similar argument as in the derivation of (3) it holds

$$\hat{p}(y|\beta x) \leq \hat{p}(i|\beta x) + \frac{1}{K}(1 - \hat{p}(i|\beta x)) = \frac{K-1}{K}\hat{p}(i|\beta x) + \frac{1}{K}. \quad (11)$$

For all  $\beta \geq \alpha$  it holds that  $\beta x \in Q_t$  so that

$$\hat{p}(i|\beta x) = \frac{1}{1 + e^{-g(\beta x)}} = \frac{1}{1 + e^{\langle W_g^{(L_g)}, U\beta x + d \rangle + b_g^{(L_g)}}}.$$

As  $x_i^{(L-1)}(x) \geq 0$  for all  $x \in \mathbb{R}^d$  it has to hold  $(\beta Ux + d)_i \geq 0$  for all  $\beta \geq \alpha$  and  $i = 1, \dots, n_{L-1}$ . This implies that  $(Ux)_i \geq 0$  for all  $i = 1, \dots, n_{L-1}$  and since  $Ux \neq 0$  there has to exist at least one component  $i^*$  such that  $(Ux)_{i^*} > 0$ . Moreover,  $W_g^{(L_g)}$  has strictly negative components and thus for all  $\beta \geq \alpha$  it holds

$$g(\beta x) = \langle W_g^{(L_g)}, U\beta x + d \rangle + b_g^{(L_g)} = \beta \langle W_g^{(L_g)}, Ux \rangle + \langle W_g^{(L_g)}, d \rangle + b_g^{(L_g)}.$$

As  $\langle W_g^{(L_g)}, Ux \rangle < 0$  we get  $\lim_{\beta \rightarrow \infty} g(x) = -\infty$  and thus

$$\lim_{\beta \rightarrow \infty} \hat{p}(i|\beta x) = 0.$$

Plugging this into (11) yields the result.  $\square$

## D Experimental Details

**Datasets** We use CIFAR10 and CIFAR100 (26) (MIT license), SVHN (37) (free for non-commercial use), LSUN (49) (no license), the ILSVRC2012 split of ImageNet (14; 43) (free for non-commercial use), FGVC-Aircraft (32) (free for non-commercial use), Stanford Cars (23) (free for non-commercial use), OpenImages v4 (27) (images have a CC BY 2.0 license), Oxford 102 Flower (39) (no license) as well as 80 million tiny images (46) (no license given, see also App. E). For the train/test splits we use the standard splits, except on 80M Tiny Images where we treat a random but fixed subset of 1000 images in the first 1,000,000 as our test set. For all datasets that get used as a test out-distribution we use a random but fixed subset of 1000 images.

Following (6), the smooth noise that is used is generated as follows. Uniform noise is generated and then smoothed using a Gaussian filter with a width that is drawn uniformly at random in  $[1, 2.5]$ . Each datapoint is then shifted and scaled linearly to ensure full range in  $[0, 1]$ , i.e.  $x' = \frac{x - \min(x)}{\max(x) - \min(x)}$ .

**Binary Training** The architecture that we use for the binary discriminator is relatively shallow (5 linear layers). The architecture is shown in Table 3. Similarly to (50; 6), we use long training schedules, running Adam for 1000 epochs, with an initial learning rate of  $1e-4$  that we decrease by a factor of 5 on epochs 500, 750 and 850 and with a batch size of 128 from the in-distribution and 128 from the out-distribution (for R.ImgNet: 50 epochs with drops at 25, 35, 45, batch sizes 32). In order to avoid large losses we also use a simple ramp up schedule for the  $\epsilon$  used in IBP and we downweight the out-distribution loss during the initial phase of training by a scalar  $\kappa$ . Both  $\epsilon$  and  $\kappa$  are increased linearly from 0 to their final values (0.01 and 1, respectively) over the first 300 epochs (for R.ImgNet over the first 25 epochs). Compared to the training of (6) which sometimes fails, we found that training of the binary classifier is very stable and even 100 epochs on CIFAR would be sufficient, but we found that longer training lead to slightly better results. Weight decay is set to  $5e-4$ , but is disabled for the weights in the final layer. As data augmentation we use AutoAugment (12) for CIFAR and simple 4 pixel crops and reflections on R.ImgNet. The strict negativity of the weights leads to a negative bias of  $g$  which can cause problems at an early stage if the  $b_g^{(L_g)}$  is initialized at 0 and thus we choose 3 as initialization. All binary classifiers were trained on single 2080Ti GPUs, managed on a SLURM cluster. Overall, the training of a provable discriminator takes around 16h on CIFAR and 44h on R.ImgNet (wall clock time including evaluations and logging on each epoch).

**Semi-Joint Training** On CIFAR we train for 100 epochs using SGD with momentum of 0.9 and a learning rate of 0.1 that drops by a factor of 10 on epochs 50, 75 and 90 (on R.ImgNet 75 epochs with drops at 30 and 60). For all datasets we train using a batch size of 128 (plus 128 out-distribution samples in the case of OE). The CIFAR experiments were run on single 2080Ti GPUs. This takes about 4h20min in wall clock time. In order to fit batches of 128 in-distribution samples and 128 out-distribution samples on R.ImgNet we had to train using 4 V100 GPUs in parallel. Because of batch normalization in multi-GPU training it is important to not simply stack the batches but to

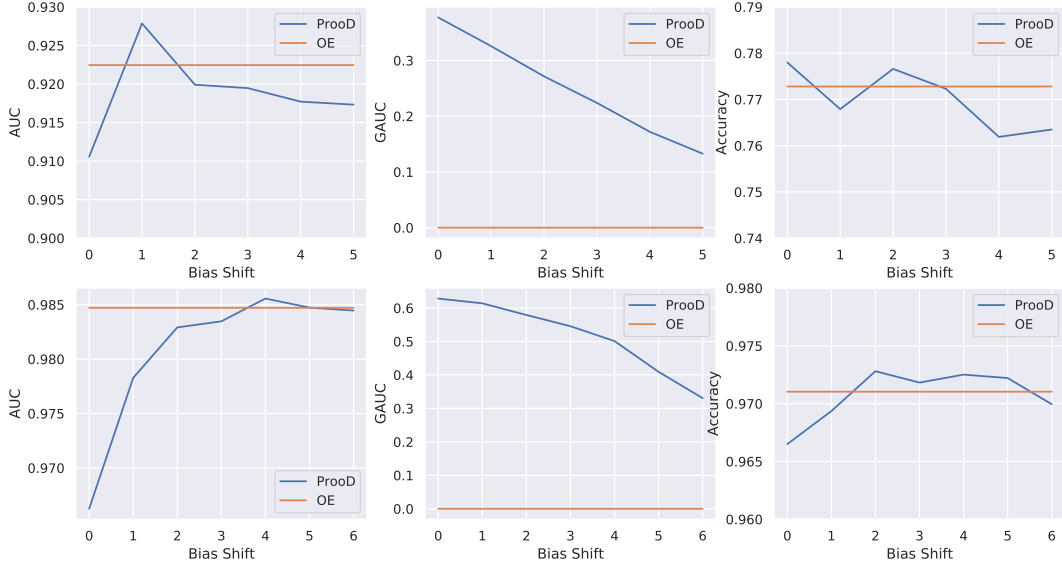


Figure 4: **Bias selection for CIFAR100 and RImgNet:** Using CIFAR100 (top) and R.ImgNet (bottom) as the in-distribution and the test set of 80M Tiny Images (or NotR.ImgNet respectively) as OOD we plot the test accuracy, AUC and GAUC as a function of the bias shift  $\Delta$  (see Eq. (8)).

interlace in- and out-distribution samples. The wall clock time was around 15h for the semi-joint training on R.ImgNet. For selecting the bias we use the procedure described in Section 4. The trade-off curves for the AUC and GAUC on CIFAR100 and R.ImgNet are given in Figure 4.

## E OpenImages as Training Out-Distribution

The 80M Tiny Images dataset has been retracted by the authors due to concerns over offensive class labels (5). Since all prior work used this dataset, we used the dataset in order to compare ProoD’s performance to prior baselines. However, we support the decision of the community to move away from the use of 80M Tiny Images, so we also trained our CIFAR models using a down-scaled version of OpenImages v4 (27) as a training out-distribution. We encourage the community to use the results in Table 5 for future comparisons.

Table 5: **Training with OpenImages:** We repeat the evaluation from Table 2 for models that were trained using OpenImages v4 as out-distribution instead of 80M Tiny Images. Plain is identical to before and is just repeated for the reader’s convenience. Note that the conclusions from the main paper still hold, which indicates that our method is robust to changes in the choice of training out-distribution.

In: CIFAR10	CIFAR100			SVHN			LSUN_CR			Smooth			
	Acc	AUC	GAUC	AAUC	AUC	GAUC	AAUC	AUC	GAUC	AAUC	AUC	GAUC	AAUC
Plain	95.01	90.0	0.0	0.6	93.8	0.0	0.1	93.1	0.0	0.5	98.2	0.0	0.6
OE	95.42	91.1	0.0	0.5	97.8	0.0	0.2	100.0	0.0	5.2	100.0	0.0	4.1
ProoD-Disc	-	62.9	57.1	57.8	72.6	65.6	66.4	78.1	71.5	72.3	59.5	50.0	50.7
ProoD $\Delta=3$	95.26	90.0	45.2	45.9	97.6	52.4	53.2	100.0	57.4	58.9	99.9	37.6	38.4
In: CIFAR100	CIFAR100			SVHN			LSUN_CR			Smooth			
	Acc	AUC	GAUC	AAUC	AUC	GAUC	AAUC	AUC	GAUC	AAUC	AUC	GAUC	AAUC
Plain	77.38	77.7	0.0	0.3	81.9	0.0	0.2	76.4	0.0	0.3	88.8	0.0	0.5
OE	77.86	77.5	0.0	0.3	89.0	0.0	0.1	100.0	0.0	0.2	99.2	0.0	0.2
ProoD-Disc	-	56.1	52.1	52.3	61.0	58.2	58.4	70.4	66.9	67.1	30.3	27.0	27.1
ProoD $\Delta=1$	77.40	75.6	30.7	30.8	86.7	34.9	35.0	100.0	40.0	40.1	99.1	16.1	16.2

## F False Positive Rates

Since in a practical setting a threshold for OOD detection ultimately has to be chosen, it can be interesting to study the false positive rate at a fixed threshold. It is relatively standard to pick the false positive rate at 95% true positive rate (called FPR in Table 6), where low values are desirable. We show the results for all methods and datasets in Table 6. Although ProoD has similarly good performance as OE on this task, it fails to give non-trivial guarantees. Therefore achieving stronger bounds on the worst-case FPR is an interesting task for future work.

**Table 6: False Positive Rates:** For all models we report accuracy on the the test of the in-distribution and the false positive rate at 95% true positive rate (FPR) (smaller is better). We also show the adversarial FPR (AFPR) and the guaranteed FPR (GFPR) for different test out-distributions. The radius of the  $l_\infty$ -ball for the adversarial manipulations of the OOD data is  $\epsilon = 0.01$  for all datasets. The bias shift  $\Delta$  that was used for ProoD is shown for each in-distribution. As discussed in Section 5, ProoD still struggles to give non-trivial guarantees for the FPR@95% on most datasets. However, different from GOOD or ProoD-Disc, the clean performance is generally as good as that of OE.

In: CIFAR10	Acc	CIFAR100			SVHN			LSUN_CR			Smooth		
		FPR	GFPR	AFPR	FPR	GFPR	AFPR	FPR	GFPR	AFPR	FPR	GFPR	AFPR
Plain	95.01	56.3	100.0	100.0	40.7	100.0	100.0	46.7	100.0	100.0	9.2	100.0	100.0
OE	95.53	20.7	100.0	99.6	1.7	100.0	100.0	1.3	100.0	99.7	0.0	100.0	96.5
ATOM	95.20	26.5	100.0	88.8	0.8	100.0	94.0	0.3	100.0	66.0	0.0	100.0	99.2
ACET	91.48	39.2	100.0	67.1	29.3	100.0	63.6	5.0	100.0	29.7	0.4	100.0	10.8
GOOD <sub>80</sub>	90.13	48.9	96.3	69.0	33.5	99.9	65.2	43.0	100.0	59.3	31.8	100.0	50.6
GOOD <sub>100</sub>	90.14	78.7	85.7	84.8	81.2	87.5	86.9	91.3	96.3	96.3	68.4	85.6	84.4
ProoD-Disc	-	78.5	83.5	83.1	69.2	79.2	78.1	86.3	93.7	92.7	82.4	93.0	91.2
ProoD $\Delta=3$	95.47	22.2	100.0	99.4	1.5	100.0	100.0	1.3	100.0	99.0	0.0	100.0	100.0
In: CIFAR100	Acc	CIFAR100			SVHN			LSUN_CR			Smooth		
		FPR	GFPR	AFPR	FPR	GFPR	AFPR	FPR	GFPR	AFPR	FPR	GFPR	AFPR
Plain	77.38	80.1	100.0	100.0	77.3	100.0	100.0	79.0	100.0	100.0	60.4	100.0	100.0
OE	77.28	73.6	100.0	100.0	40.0	100.0	100.0	14.0	100.0	100.0	12.6	100.0	100.0
ATOM	75.06	88.9	100.0	99.9	37.7	100.0	100.0	8.7	100.0	98.0	0.0	100.0	100.0
ACET	74.43	79.1	100.0	100.0	53.5	100.0	100.0	21.3	100.0	100.0	49.4	100.0	100.0
ProoD-Disc	-	97.9	98.4	98.4	86.7	89.3	89.1	96.0	98.0	97.7	99.2	99.2	99.2
ProoD $\Delta=1$	76.79	77.7	100.0	100.0	36.4	100.0	100.0	15.3	100.0	100.0	1.6	100.0	100.0
In: R.ImgNet	Acc	Flowers			FGVC			Cars			Smooth		
		FPR	GFPR	AFPR	FPR	GFPR	AFPR	FPR	GFPR	AFPR	FPR	GFPR	AFPR
Plain	96.34	55.2	100.0	100.0	48.2	100.0	100.0	75.2	100.0	100.0	0.0	100.0	100.0
OE	97.10	18.2	100.0	100.0	0.2	100.0	100.0	0.0	100.0	100.0	0.0	100.0	100.0
ProoD-Disc	-	59.2	65.2	65.0	51.0	67.8	66.5	51.7	63.7	62.3	100.0	100.0	100.0
ProoD $\Delta=4$	97.25	18.5	100.0	100.0	0.5	100.0	100.0	0.0	100.0	100.0	0.0	100.0	100.0

## G Additional Datasets

In addition to the results shown in Table 2, it is interesting to study how ProoD performs on uniform noise as well as the test set of out-distribution it was trained on. We show the results in Table 7. As in Table 2 the clean performance of ProoD is comparable to that of OE, but it achieves non-trivial GAUC. On CIFAR10, GOOD<sub>100</sub> achieves almost perfect GAUC against uniform noise, which comes at the price of significantly worse clean AUCs on all other out-distributions, see Table 2.

## H Error Bars

In order to be mindful of our resource consumption we restrict the computation of error bars to our experiments on CIFAR10. We rerun our experiments using the same hyperparameters 5 times. We compute the mean and the standard deviations for our models for all metrics shown in Table 2. The

Table 7: **Additional Datasets:** We show the AUC, AAUC and GAUC for all models on uniform noise and on the test set of the train out-distribution.

In: CIFAR10	Uniform				Tiny Images		
	Acc	AUC	GAUC	AAUC	AUC	GAUC	AAUC
Plain	95.01	98.0	0.0	82.9	91.7	0.0	0.7
OE	95.53	99.5	0.0	88.0	98.7	0.0	11.1
ATOM	92.33	99.9	0.0	99.9	98.7	0.0	37.4
ACET	91.48	99.9	0.0	99.9	97.1	0.0	92.1
GOOD <sub>80</sub>	90.13	95.8	95.3	95.5	92.4	56.1	78.4
GOOD <sub>100</sub>	90.14	99.5	99.0	99.2	81.5	68.1	68.1
ProoD-Disc	-	99.7	99.6	99.6	80.1	75.5	75.7
ProoD $\Delta=3$	95.47	99.2	80.4	90.1	98.5	52.8	56.0
In: CIFAR100	Uniform				Tiny Images		
	Acc	AUC	GAUC	AAUC	AUC	GAUC	AAUC
Plain	77.38	82.2	0.0	53.0	81.7	0.0	0.9
OE	77.28	95.8	0.0	64.1	92.2	0.0	4.0
ATOM	71.72	100.0	0.0	100.0	91.9	0.0	11.5
ACET	74.43	99.4	0.0	97.5	91.9	0.0	3.8
ProoD-Disc	-	98.9	98.8	98.8	68.7	65.0	65.4
ProoD $\Delta=1$	76.79	97.4	57.2	76.1	92.8	32.6	33.0
In: R.ImgNet	Uniform				NotR.ImgNet		
	Acc	AUC	GAUC	AAUC	AUC	GAUC	AAUC
Plain	96.34	99.3	0.0	74.9	91.7	0.0	0.2
OE	97.10	99.6	0.0	84.6	98.7	0.0	1.2
ProoD-Disc	-	99.7	99.2	99.3	73.6	69.9	69.9
ProoD $\Delta=4$	97.25	99.8	79.7	95.2	98.6	50.1	51.3

results are shown in Table 8. We see that the fluctuations across different runs are indeed rather small. Furthermore, the clean performance of OE and ProoD show no significant discrepancies.

Table 8: **Error Bars:** We show the mean and standard deviation  $\sigma$  of all metrics for our CIFAR10 models across 5 runs. The tolerances for ProoD’s clean performance are very small and yet the differences in clean performance between OE ProoD are not significant.

In: CIFAR10	CIFAR100				SVHN				LSUN_CR				Smooth			
	Acc	AUC	GAUC	AAUC	AUC	GAUC	AAUC	AUC	GAUC	AAUC	AUC	GAUC	AAUC	AUC	GAUC	AAUC
Plain	94.91	90.0	0.0	0.6	93.9	0.0	0.1	93.4	0.0	0.7	96.7	0.0	1.2			
Plain $\sigma$	0.16	0.1	0.0	0.1	1.2	0.0	0.0	0.3	0.0	0.2	2.1	0.0	0.5			
OE	95.56	96.1	0.0	7.6	99.4	0.0	0.4	99.6	0.0	16.7	99.6	0.0	4.3			
OE $\sigma$	0.04	0.1	0.0	1.5	0.1	0.0	0.2	0.1	0.0	3.5	0.3	0.0	3.7			
ProoD-Disc	-	67.7	61.6	62.2	75.5	68.6	69.3	76.5	70.4	70.9	87.2	77.7	78.8			
ProoD-Disc $\sigma$	-	0.7	0.7	0.7	1.4	1.7	1.5	1.4	1.7	1.7	3.6	4.3	4.3			
ProoD $\Delta=3$	95.60	96.0	42.2	44.1	99.4	48.6	49.2	99.6	47.1	52.0	99.8	55.2	57.0			
ProoD $\Delta=3 \sigma$	0.11	0.1	0.8	0.8	0.1	0.6	0.6	0.1	1.5	1.9	0.1	2.9	3.4			